J. Austral. Math. Soc. (Series B) 23 (1981), 103–114

EFFECTS OF IRON ON A TOROIDAL CONDUCTOR

JAMES CALDWELL

(Received 24 April 1979)

(Revised 10 March 1980)

Abstract

The effects of iron on the uniformity of the field produced by a current-carrying axisymmetric conductor are considered. Using a perturbation analysis a simple analytic expression is obtained which describes the field close to the axis of symmetry. A Fourier series approach is also used to provide an analytical solution to the problem and the accuracy of the perturbation method is estimated by comparing results.

1. Introduction and governing equations

Calculations of the magnetostatic field associated with iron-free axisymmetric systems have received much attention in the literature (see, for example, Boom and Livingston [2] and Garrett [3] where earlier references may be found). However, in past work little account has been taken of the effects of the presence of magnetic material on such systems. The introduction of iron has obvious advantages since it clearly provides more field for the same current and hence ensures substantial power savings for conventional conductors. Furthermore, placing the iron in a suitable position will improve field uniformity even for superconducting magnets. In this paper the effects of iron on the uniformity of the field produced by a current-carrying axisymmetric conductor are considered. To this end the field uniformity is examined as a function of the inner and outer radii of the conductor. In Section 2 a simple analytic expression which describes the field in the neighbourhood of the axis of symmetry is obtained.

The geometry to be considered is shown in Figure 1. A toroidal conductor region V' of rectangular cross-section, having inner radius A, outer radius B and length $(L - 2\eta)$, is located midway between two semi-infinite regions of iron, distance L apart, the axis of symmetry of the torus being perpendicular to the iron boundaries. The region V between the conductor and iron is assumed to be insulating. For convenience normalized units based on L are used. Thus $a = A/L$ is used for the inner radius, $b = B/L$ for the outer radius and $\varepsilon = \eta/L$ for the distance between the conductor and the iron (see Fig. 1). Cylindrical polar coordinates (r, ϕ, z) are employed where r and z are normalized in terms of L.

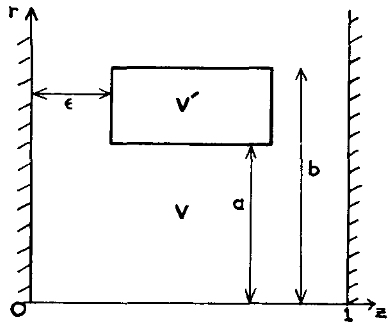

Figure 1.

Since the conductor carries a prescribed current density λ' in the azimuthal direction, Ampère's law implies

$$\operatorname{curl} \mathbf{B} = \mathbf{0} \quad \text{in } V, \tag{1}$$

$$\operatorname{curl} \mathbf{B} = \lambda \mathbf{1}_\phi \quad \text{in } V', \ (\mu \text{ constant}), \tag{2}$$

where $\lambda = \lambda' L^2$ and $\mathbf{1}_\phi$ is a unit vector in the direction of increasing ϕ. Also, by continuity,

$$\operatorname{div} \mathbf{B} = 0 \quad \text{in } V \text{ and } V'. \tag{3}$$

Clearly $\mathbf{B}$ must lie in meridional planes and so

$$\mathbf{B} = (B_r(r, z), 0, B_z(r, z)), \tag{4}$$

where the given axisymmetry has been employed. Equation (4) suggests the introduction of vector potential A_ϕ which satisfies equation (3) identically:

$$B_r(r, z) = -\frac{\partial A_\phi}{\partial z} \quad \text{and} \quad B_z(r, z) = \frac{1}{r}\frac{\partial}{\partial r}(rA_\phi). \tag{5}$$

It then follows that

$$\operatorname{curl} \mathbf{B} = -\mathbf{1}_\phi \nabla_1^2 A_\phi, \tag{6}$$

where

$$\nabla_1^2 = \frac{\partial^2}{\partial r^2} + \frac{1}{r}\frac{\partial}{\partial r} - \frac{1}{r^2} + \frac{\partial^2}{\partial z^2}. \tag{7}$$

Equations (1) and (2) then become

$$\nabla_1^2 A_\phi = 0 \quad \text{in } V, \tag{8}$$

and

$$\nabla_1^2 A_\phi = -\lambda \quad \text{in } V'. \tag{9}$$

Since the walls $z = 0, 1$ have infinite permeability then

$$\mathbf{n} \times \mathbf{B} = \mathbf{0} \quad \text{on } z = 0 \text{ and } z = 1, \tag{10}$$

where $\mathbf{n}$ is the unit vector normal to the walls, that is,

$$\frac{\partial A_\phi}{\partial z} = 0 \quad \text{on } z = 0 \text{ and } z = 1. \tag{11}$$

See later for the case of finite permeability. The conditions that A_ϕ remains bounded imply that

$$A_\phi = 0 \quad \text{on } r = 0, \tag{12}$$

and finally

$$A_\phi \to 0 \quad \text{as } r \to \infty. \tag{13}$$

These equations are solved by a perturbation analysis in Section 2 and by a Fourier series approach in Section 3, and the accuracy is estimated by comparing the results.

2. Perturbation analysis

If $\varepsilon = 0$ then the field would, in fact, be everywhere parallel to the axis; furthermore, it could be argued that to obtain fields which are approximately uniform in the neighbourhood of the axis it is necessary that $\varepsilon \ll 1$. This suggests that useful results may be obtained by a perturbation scheme using ε as a small parameter.

Setting $\varepsilon = 0$, the governing equations (8) and (9) become

$$\frac{d^2\psi_0}{dr^2} + \frac{1}{r}\frac{d\psi_0}{dr} - \frac{\psi_0}{r^2} = \begin{cases} 0 & \text{for } r < a \text{ and } r > b, \\ -\lambda & \text{for } a < r < b. \end{cases} \tag{14}$$

Note that, as $A_\phi = \psi_0(r)$, equation (11) is automatically satisfied. Appealing to equations (12) and (13) the required solution of (14) is

$$\psi_0 = \begin{cases} lr & \text{for } r < a, \\ -\dfrac{\lambda r^2}{3} + mr + \dfrac{n}{r} & \text{for } a < r < b, \\ \dfrac{p}{r} & \text{for } r > b, \end{cases} \tag{15}$$

https://doi.org/10.1017/S0334270000000096 Published online by Cambridge University Press

where l, m, n and p are arbitrary constants to be determined by the continuity of A_ϕ and dA_ϕ/dr at $r = a$ and $r = b$. The solution gives

$$\psi_0 = \lambda(b-a)r/2 \quad \text{for } r < a. \tag{16}$$

The differential system posed by equations (8), (9), (11), (12) and (13) is solved by writing

$$A_\phi = \psi_0 + \Psi \tag{17}$$

and introducing a system of image coils in the usual way.

It then follows that the solution is

$$\Psi = -\frac{\lambda}{4\pi}\int_a^b\int_0^{2\pi}\int_{-\varepsilon}^{\varepsilon}\sum_{n=-\infty}^{\infty}\frac{x\cos\theta\,dx\,d\theta\,dz'}{\left[(z-z'-n)^2+r^2+x^2-2xr\cos\theta\right]^{1/2}} \tag{18}$$

which will give the field near the axis if evaluated for small r. Thus

$$\begin{aligned}\Psi &= -\frac{r\lambda}{4}\int_a^b\int_{-\varepsilon}^{\varepsilon}\sum_{n=-\infty}^{\infty}\frac{x^2\,dx\,dz'}{\left[(z-z'-n)^2+x^2\right]^{3/2}} + O(r^3)\\ &= -\frac{r\lambda}{4}\int_{-\varepsilon}^{\varepsilon}\sum_{n=-\infty}^{\infty}\left[\frac{1}{2}\ln\left(\frac{1+\sin\phi}{1-\sin\phi}\right)-\sin\phi\right]_{x=a}^{x=b}dz' + O(r^3),\end{aligned}$$

where $\phi = \tan^{-1}(x/(z-z'-n))$. It is important to note that this formula is correct to $O(r^3)$, which suggests it will be accurate in the neighbourhood of the axis. Finally, the above formula can be simplified by assuming that ε is small, as it will be in practice. It then follows that

$$\Psi = -\frac{\varepsilon r\lambda}{2}\sum_{n=-\infty}^{\infty}\left[\frac{1}{2}\ln\left(\frac{1+\sin\phi}{1-\sin\phi}\right)-\sin\phi\right]_{x=a}^{x=b} + O(\varepsilon^3),$$

where, in this case, $\phi = \tan^{-1}(x/(z-n))$. Hence

$$\Psi = -\frac{\varepsilon r\lambda}{2}\left[F(b,z)-F(a,z)\right] + O(\varepsilon^3), \tag{19}$$

where

$$F(c,z) = \sum_{n=-\infty}^{\infty}\left[\frac{1}{2}\ln\left(\frac{1+\sin\phi}{1-\sin\phi}\right)-\sin\phi\right] \tag{20}$$

and

$$\sin\phi = \frac{c}{\left[(z-n)^2+c^2\right]^{1/2}}.$$

Note again that equation (19) is correct to $O(\varepsilon^3)$, which suggests that it will be accurate.

This means that

$$A_\phi = \frac{1}{2}\lambda(b-a)r + -\frac{\varepsilon\lambda r}{2}\left[F(b,z)-F(a,z)\right] + O(\varepsilon^3), \tag{21}$$

where the first term on the right hand side corresponds to uniform field and the second term gives a measure of the contribution from other fields which are non-uniform.

It then follows from equation (21) that

$$B_z = \frac{1}{r}\frac{\partial}{\partial r}(rA_\phi) = \lambda(b-a) - \varepsilon\lambda\left[F(b,z) - F(a,z)\right]. \tag{22}$$

Note that, as $\varepsilon \to 0$, $B_z \to \lambda(b-a) = B_0$, say. A precise measure of the deviation from uniform field is then given by

$$\frac{1}{B_0}\frac{\partial B_z}{\partial z} = -\frac{\varepsilon}{b-a}\frac{\partial}{\partial z}\left[F(b,z) - F(a,z)\right].$$

From equation (20)

$$F(c,z) = \sum_{n=1}^{\infty}\left[f(n) + f(-n)\right] + \frac{1}{2}\ln\frac{(z^2+c^2)^{1/2}+c}{(z^2+c^2)^{1/2}-c} - \frac{c}{(z^2+c^2)^{1/2}}, \tag{23}$$

where

$$f(n) = \frac{1}{2}\ln\frac{\left[(z-n)^2+c^2\right]^{1/2}+c}{\left[(z-n)^2+c^2\right]^{1/2}-c} - \frac{c}{\left[(z-n)^2+c^2\right]^{1/2}}. \tag{24}$$

Clearly the series $\Sigma f(n)$ and $\Sigma f(-n)$ are slowly convergent. Because of this slow convergence it is not sufficient to consider a model consisting of 2 or 3 images.

In the neighbourhood of the axis of symmetry, the field B_z can now be obtained from a simple analytic expression obtained by substituting this expression for $F(c, z)$ in equation (22). Hence it is possible to investigate the effects of the variation of the coil geometry on the field uniformity.

The summations $\Sigma_{n=1}^{N} f(n)$ and $\Sigma_{n=1}^{N} f(-n)$ have been carried out directly for the cases $N = 100$ and $N = 200$. As a result, values of $F(c, z)$ have been computed for $c = 0.8(0.1)1.8$ and $z = 0.4$ and 0.5 and are presented in Table 1. The results for $N = 100$ and 200 differ by at most 0.005%.

As has been noted earlier the above analysis applies for infinite permeability μ. The case of finite permeability may be treated in a similar manner but with each term of the series for $F(c, z)$ containing as a factor a power of the image factor $(\mu - 1)/(\mu + 1)$. By comparing the new summations with the original values it is found that, for $\mu > 100$, the values in Table 1 are affected only in the sixth decimal place. This conclusion could have useful application.

TABLE 1

Computed values of $F(c, z)$ for $c = 0.8(0.1)1.8$, $z = 0.4$, 0.5 and $N = 100,200$.

c	$F(c, 0.4)$ $N = 100$	$F(c, 0.4)$ $N = 200$	$F(c, 0.5)$ $N = 100$	$F(c, 0.5)$ $N = 200$
0.8	0.967987	0.968000	0.920359	0.920372
0.9	1.116314	1.163154	1.114389	1.114407
1.0	1.360408	1.360433	1.311027	1.311052
1.1	1.558879	1.558912	1.509142	1.509175
1.2	1.758021	1.758064	1.708086	1.708128
1.3	1.957538	1.957592	1.907492	1.907546
1.4	2.157261	2.157329	2.107154	2.107221
1.5	2.357097	2.347181	2.306956	2.307040
1.6	2.556995	2.557096	2.506836	2.506937
1.7	2.756925	2.757046	2.706755	2.706877
1.8	2.956871	2.957015	2.906696	2.906840

3. Fourier series approach

The differential system posed by equations (8), (9), (11), (12) and (13) may be solved by examining Fourier type solutions. In order to introduce symmetry it is more convenient to locate the iron boundaries at $z = -1$ and $+1$ instead of at $z = 0$ and 1. This means that equation (11) is replaced by

$$\frac{\partial A_\phi}{\partial z} = 0 \qquad \text{on } z = \pm 1. \tag{25}$$

Because of the given symmetry the solutions are periodic (with period 2) of Fourier cosine form, namely

$$A_\phi(r, z) = f_0(r) + \sum_{n=1}^{\infty} f_n(r) \cos n\pi z. \tag{26}$$

Assuming equation (26), we obtain the following complementary functions:

(a) $f_0(r) = r$ and $\frac{1}{r}$

and

(b) $f_n(r) = I_1(n\pi r)$ and $K_1(n\pi r)$ for $n \neq 0$,

where I_1 and K_1 are the modified Bessel functions. Thus we have

$$A_\phi = a_0 r + \sum_{n=1}^{\infty} a_n I_1(n\pi r) \cos n\pi z \quad \text{for } r < a \tag{27}$$

and

$$A_\phi = \frac{d_0}{r} + \sum_{n=1}^{\infty} d_n K_1(n\pi r) \cos n\pi z \quad \text{for } r > b, \tag{28}$$

https://doi.org/10.1017/S0334270000000096 Published online by Cambridge University Press

which satisfy the conditions of boundedness. The complementary function for $a < r < b$ is

$$A_\phi = b_0 r + c_0/r + \sum_{n=1}^{\infty} \{b_n I_1(n\pi r) + c_n K_1(n\pi r)\}\cos n\pi z. \tag{29}$$

To obtain the particular integral we must first Fourier analyse the square wave given by

$$g(z) = \begin{cases} -\lambda & \text{for } 0 < z < 1 - 2\varepsilon, \\ 0 & \text{for } 1 - 2\varepsilon < z < 1, \end{cases}$$

and

$$g(z + 2) = g(z).$$

Note that ε is replaced by 2ε to maintain the consistency with the geometry in Figure 1 now that we are using period 2. This leads to

$$g(z) = \lambda(2\varepsilon - 1) + \frac{2\lambda}{\pi} \sum_{n=1}^{\infty} \frac{(-1)^n}{n} \sin 2n\pi\varepsilon \cos n\pi z. \tag{30}$$

For the $n = 0$ case we require the particular integral of

$$\left(\frac{1}{r}\frac{d}{dr}r\frac{d}{dr} - \frac{1}{r^2}\right)P_0(r) = \lambda(2\varepsilon - 1),$$

which is

$$P_0(r) = \frac{\lambda(2\varepsilon - 1)r^2}{3}.$$

For $n \neq 0$ we have

$$\left(\frac{1}{r}\frac{d}{dr}r\frac{d}{dr} - \frac{1}{r^2} - n^2\pi^2\right)P_n(r) = \frac{2\lambda(-1)^n}{\pi n} \sin 2n\pi\varepsilon,$$

which reduces to

$$\left(\frac{1}{x}\frac{d}{dx}x\frac{d}{dx} - \frac{1}{x^2} - 1\right)p_n(x) = 1 \tag{31}$$

if we let $x = n\pi r$ and

$$P_n(r) = \frac{2\lambda(-1)^n}{(\pi n)^3} \sin 2n\pi\varepsilon\, p_n(x). \tag{32}$$

We now obtain the particular integral of (31) by variation of parameters, that is

$$p_n(x) = A(x)I_1(x) + B(x)K_1(x),$$

where we assume

$$A'(x)I_1(x) + B'(x)K_1(x) = 0,$$

https://doi.org/10.1017/S0334270000000096 Published online by Cambridge University Press

and by substitution

$$A'(x)I_1'(x) + B'(x)K_1'(x) = 1.$$

Thus we have

$$A'(x)\{I_1'(x)K_1(x) - I_1(x)K_1'(x)\} = K_1(x)$$

and

$$B'(x)\{I_1(x)K_1'(x) - K_1(x)I_1'(x)\} = I_1(x).$$

Now the Wronskian $I_1(x)K_1'(x) - K_1(x)I_1'(x) = -1/x$ (refer to Watson [5]), which gives

$$A(x) = \int^x xK_1(x)\,dx, \qquad B(x) = -\int^x xI_1(x)\,dx,$$

and hence

$$p_n(x) = I_1(x)\int^x tK_1(t)\,dt - K_1(x)\int^x tI_1(t)\,dt.$$

This means that from equation (32)

$$P_n(r) = \frac{2\lambda(-1)^n}{\pi^3 n^3}\sin 2n\pi\varepsilon\left\{I_1(n\pi r)\int_{n\pi a}^{n\pi r} tK_1(t)\,dt - K_1(n\pi r)\int_{n\pi a}^{n\pi r} tI_1(t)\,dt\right\}. \tag{33}$$

Thus the complete set of solutions is as follows:

$$\text{(a)}\quad A_\phi = a_0 r + \sum_{n=1}^{\infty} a_n I_1(n\pi r)\cos n\pi z \qquad \text{for } r < a, \tag{34}$$

$$\begin{aligned}\text{(b)}\quad A_\phi = {} & b_0 r + \frac{c_0}{r} + \sum_{n=1}^{\infty}\{b_n I_1(n\pi r) + c_n K_1(n\pi r)\}\cos n\pi z \\ & + \frac{\lambda(2\varepsilon - 1)r^2}{3} + \frac{2\lambda}{\pi^3}\sum_{n=1}^{\infty}\frac{(-1)^n}{n^3}\sin 2n\pi\varepsilon \\ & \cdot\left\{I_1(n\pi r)\int_{n\pi a}^{n\pi r} tK_1(t)\,dt - K_1(n\pi r)\int_{n\pi a}^{n\pi r} tI_1(t)\,dt\right\} \quad \text{for } a < r < b,\end{aligned} \tag{35}$$

and

$$\text{(c)}\quad A_\phi = \frac{d_0}{r} + \sum_{n=1}^{\infty} d_n K_1(n\pi r)\cos n\pi r \quad \text{for } r > b. \tag{36}$$

To solve for a_n, b_n, c_n and d_n we match A_ϕ and $\partial A_\phi/\partial r$ at $r = a$ and b and compare coefficients of $\cos n\pi z$ for $n = 0, 1, \ldots$. For the $n = 0$ case the following equations clearly apply:

$$a_0 a = b_0 a + (c_0/a) + (\lambda(2\varepsilon - 1)a^2)/3,$$

$$a_0 = b_0 - (c_0/a^2) + (2\lambda(2\varepsilon - 1)a)/3,$$

$$d_0/b = b_0 b + (c_0/b) + (\lambda(2\varepsilon - 1)b^2)/3,$$

https://doi.org/10.1017/S0334270000000096 Published online by Cambridge University Press

and

$$-d_0/b^2 = b_0 - \left(c_0/b^2\right) + (2\lambda(2\varepsilon - 1)b)/3,$$

and hence

$$a_0 = \frac{\lambda(2\varepsilon - 1)(a - b)}{2}. \tag{37}$$

For $n \neq 0$ we have

$$\begin{aligned}
a_n I_1(n\pi a) &= b_n I_1(n\pi a) + c_n K_1(n\pi a), \\
a_n I_1'(n\pi a) &= b_n I_1'(n\pi a) + c_n K_1'(n\pi a), \\
d_n K_1(n\pi b) &= b_n I_1(n\pi b) + c_n K_1(n\pi b) \\
&\quad + \frac{2\lambda(-1)^n}{\pi^3 n^3} \sin 2n\pi\varepsilon \left\{ I_1(n\pi b) \int_{n\pi a}^{n\pi b} t K_1(t)\, dt \right. \\
&\qquad \left. - K_1(n\pi b) \int_{n\pi a}^{n\pi b} t I_1(t)\, dt \right\},
\end{aligned}$$

and

$$\begin{aligned}
d_n K_1'(n\pi b) &= b_n I_1'(n\pi b) + c_n K_1'(n\pi b) \\
&\quad + \frac{2\lambda(-1)^n}{\pi^3 n^3} \sin 2n\pi\varepsilon \left\{ I_1'(n\pi b) \int_{n\pi a}^{n\pi b} t K_1(t)\, dt \right. \\
&\qquad \left. - K_1'(n\pi b) \int_{n\pi a}^{n\pi b} t I_1(t)\, dt \right\}.
\end{aligned}$$

Eliminating d_n and using the Wronskian gives

$$b_n = -\frac{2\lambda(-1)^n \sin 2n\pi\varepsilon}{\pi^3 n^3} \int_{n\pi a}^{n\pi b} t K_1(t)\, dt, \tag{38}$$

where

$$\begin{aligned}
\int_{n\pi a}^{n\pi b} t K_1(t)\, dt = \frac{n\pi^2}{2} \big[& b\{K_1(n\pi b) L_0(n\pi b) - L_1(n\pi b) K_0(n\pi b)\} \\
& - a\{K_1(n\pi a) L_0(n\pi a) - L_1(n\pi a) K_0(n\pi a)\} \big]
\end{aligned} \tag{39}$$

(refer to McLachlan [4]), and L_0 and L_1 are the modified Struve functions of order 0 and 1, respectively.

Similarly, $c_n = 0$ and $a_n = b_n$. Thus, for $r < a$, we have the solution

$$A_\phi = \frac{\lambda(2\varepsilon - 1)(a - b)r}{2} - \frac{\lambda}{\pi} \sum_{n=1}^{\infty} \frac{(-1)^n \sin 2n\pi\varepsilon}{n^2} I_1(n\pi r) \cos n\pi z\, C_n(a, b), \tag{40}$$

where

$$\begin{aligned}
C_n(a, b) = & b\{K_1(n\pi b) L_0(n\pi b) - L_1(n\pi b) K_0(n\pi b)\} \\
& - a\{K_1(n\pi a) L_0(n\pi a) - L_1(n\pi a) K_0(n\pi a)\}.
\end{aligned}$$

https://doi.org/10.1017/S0334270000000096 Published online by Cambridge University Press

4. Comparison of results

The differential system has been solved by using both the perturbation and Fourier series methods in an attempt to establish the accuracy of the methods. Using the notation in Fig. 1, results have been obtained for the following sets of parameters:

(1) $\varepsilon = 0.1$, $a = 1$, $b = 1.3$;
(2) $\varepsilon = 0.2$, $a = 1$, $b = 1.3$;
(3) $\varepsilon = 0.05$, $a = 0.9$, $b = 1.1$.

TABLE 2

Comparison of the perturbation and Fourier series results for the case $\varepsilon = 0.1$, $a = 1$, $b = 1.3$ ($z = \frac{1}{2}$).

r	A (Pert.)	A (Fourier)	Percentage error in A (Pert.)
0	0	0	0
$\frac{1}{16}$	0.7511	0.7495	0.21
$\frac{1}{8}$	1.5022	1.4991	0.21
$\frac{3}{16}$	2.2533	2.2486	0.21
$\frac{1}{4}$	3.0044	2.9978	0.22

TABLE 3

Comparison of the perturbation and Fourier series results for the case $\varepsilon = 0.2$, $a = 1$, $b = 1.3$ ($z = \frac{1}{2}$).

r	A (Pert.)	A (Fourier)	Percentage error in A (Pert.)
0	0	0	0
$\frac{1}{16}$	0.5647	0.5616	0.55
$\frac{1}{8}$	1.1294	1.1231	0.56
$\frac{3}{16}$	1.6941	1.6845	0.57
$\frac{1}{4}$	2.2588	2.2463	0.56

https://doi.org/10.1017/S0334270000000096 Published online by Cambridge University Press

TABLE 4

Comparison of the perturbation and Fourier series results for the case $\varepsilon = 0.05$, $a = 0.9$, $b = 1.1$ ($z = \frac{1}{2}$).

r	A (Pert.)	A (Fourier)	Percentage error in A (Pert.)
0	0	0	0
$\frac{1}{16}$	0.5633	0.5623	0.18
$\frac{1}{8}$	1.1266	1.1246	0.18
$\frac{3}{16}$	1.6899	1.6869	0.18
$\frac{1}{4}$	2.2532	2.2493	0.17

In using the Fourier series approach the required values of $I_1(x)$, $K_1(x)$, $L_0(x)$ and $L_1(x)$ were obtained from Abramowitz and Stegun [1]. For the three cases listed above results correct to four decimal places were obtained by taking the first five terms in the series in equation (40). Later terms decrease rapidly in magnitude and do not affect the fourth decimal place. These results can be compared to the perturbation solution given by equation (21) where λ has been taken as 100 and the function values $F(z, z)$ and $F(b, z)$ are obtained from Table 1. In fact, a comparison has been carried out for the case $z = 0.5$ (which corresponds to $z = 0$ in equation (40)) when the radius $r = 0\ (\frac{1}{16})\frac{1}{4}$ (see Tables 2, 3 and 4).

Clearly the agreement is good and this gives us confidence in the perturbation approach. As pointed out in the tables, the maximum error in the perturbation results is well below 1% for all three cases considered.

In the perturbation method the known solution ψ_0 of the zero air gap case with infinite permeability μ is used as a starting value and corrections are made to take into account the effect of finite air gap and finite permeability. In this way a good solution is obtained even for an approximate estimation of the correction. The method clearly has some merit particularly for large permeability μ and could be applied to other field problems. For the particular problem considered it is rather fortuitous that an analytical solution in terms of modified Bessel and Struve functions is possible. This will not always be so but is important here as a check in that it convinces us of the merit of the perturbation approach which provides us with a simple analytic expression from which the field close to the axis of symmetry can be found with comparatively little computing effort. As mentioned earlier the perturbation method has wider application.

Acknowledgement

The author would like to thank Professor R. D. Gibson (Newcastle upon Tyne Polytechnic) for both his help and interest in this work.

References

[1] M. Abramowitz and I. A. Stegun, *Handbook of mathematical functions* (Dover, New York, 1965).
[2] R. W. Boom and R. S. Livingston, "Superconducting solenoids", *Proc. I.R.E.* (1962), 274–285.
[3] M. W. Garrett, "Axially symmetric systems for generating and measuring magnetic fields. Part I," *J. Appl. Phys.* (1951), 1091–1107.
[4] N. W. McLachlan, *Bessel functions for engineers* (Clarendon Press, Oxford, 1961), p. 118.
[5] G. N. Watson, *A treatise on the theory of Bessel functions* (University Press, Cambridge, 1952), p. 80.

Department of Mathematics and Computer Studies
Sunderland Polytechnic
Sunderland
England